Molecular Therapy
Nucleic Acids
Original Article

Delivery of Cell-Specific Aptamers to the Arterial Wall with an Occlusion Perfusion Catheter

Ofonime Udofot,[1,2,11] Li-Hsien Lin,[1,11] William H. Thiel,[1] Megan Erwin,[6] Emily Turner,[6] Francis J. Miller, Jr.,[3,4,5] Paloma H. Giangrande,[1,2,7,8,9,10] and Saami K. Yazdani[6]

[1]Internal Medicine, University of Iowa, Iowa City, IA, USA; [2]Abboud Cardiovascular Research Center, University of Iowa, Iowa City, IA, USA; [3]Department of Medicine, Duke University, Durham, NC, USA; [4]Pharmacology and Cancer Biology Program, Duke University, Durham, NC, USA; [5]Department of Medicine, Veterans Administration Medical Center, Durham, NC, USA; [6]Mechanical Engineering Department, University of South Alabama, Mobile, AL, USA; [7]Holden Comprehensive Cancer Center, University of Iowa, Iowa City, IA, USA; [8]Radiation Oncology, University of Iowa, Iowa City, IA, USA; [9]Molecular & Cellular Biology Program, University of Iowa, Iowa City, IA, USA; [10]Environmental Health Sciences Research Center (EHSRC), University of Iowa, Iowa City, IA, USA

Current strategies to prevent restenosis following endovascular treatment include the local delivery of anti-proliferative agents to inhibit vascular smooth muscle cell (VSMC) proliferation and migration. These agents, not specific to VSMCs, are deposited on the luminal surface and therefore target endothelial cells and delay vascular healing. Cell-targeted therapies, (e.g., RNA aptamers), can potentially overcome these safety concerns by specifically binding to VSMC and inhibiting proliferation and migration. The purpose of this study was to therefore demonstrate the ability of a perfusion catheter to deliver cell-specific RNA aptamer inhibitors directly to the vessel wall. RNA aptamers specific to VSMCs were developed using an *in vitro* cell-based systematic evolution of ligand by exponential enrichment selection process. Two aptamers (Apt01 and Apt14) were evaluated *ex vivo* using harvested pig arteries in a pulsatile flow bioreactor. Local drug delivery of the aptamers into the medial wall was accomplished using a novel perfusion catheter. We demonstrated the feasibility to deliver aptamer-based drugs directly to the medial layer of an artery using a perfusion catheter. Such cell-specific targeted therapeutic drugs provide a potentially safer and more effective treatment option for patients with vascular disease.

INTRODUCTION

Cardiovascular disease, the primary cause of death and morbidity in the Western world, accounts for nearly 800,000 deaths yearly in the US.[1] The total cost of cardiovascular disease is estimated to more than $300 billion each year. Atherosclerosis is the primary cause of cardiovascular disease, resulting in inflammation and narrowing of arteries and potentially life-threatening complications such as stroke, heart attack, and peripheral disease. Percutaneous revascularization (balloon angioplasty and stenting) is the preferred therapy of narrowed arteries due to reduced cost, morbidity, mortality, and in-hospital stay as compared to vascular bypass surgery.[2] Unfortunately, the success of bare metal stents (BMSs) and uncoated balloon angioplasty is limited by the migration and proliferation of vascular smooth muscle cells (VSMCs) into the intima leading to high rates of restenosis (reocclusion).[3,4] Currently, the only available therapy to directly prevent VSMC proliferation is to coat stents and balloons with anti-proliferative drugs such as paclitaxel or limus (sirolimus, zotarolimus, everolimus, etc.).[5–7] However, these drugs are not selective in their suppression of VSMC growth and also inhibit endothelial cell (EC) proliferation.[8] Therefore, it is not surprising that late stent thrombosis, a rare but life-threatening complication of drug-eluting stents (DESs), has emerged as a major safety concern.[9] Autopsy studies have demonstrated that the most powerful predictor of stent thrombosis is endothelial coverage.[10]

Additionally, the prevalence of neoatherosclerosis is increased in DES autopsy cases, suggesting that long-term adverse impact of impaired vascular healing could lead to accelerated progression of atherosclerosis.[11] To overcome these limitations, the ideal therapy would deliver a VSMC-specific drug directly into the medial layer, not hindering the natural reendothelialization and vascular healing process.

We have previously shown a VSMC-targeted RNA aptamer delivered in a mixture of pluronic gel blocks cell migration and inhibits neointimal formation in a murine model of carotid injury.[12] Nucleic acid aptamers represent an emerging class of pharmaceuticals under development for diagnostic and therapeutic use.[13] Aptamers routinely achieve

Received 6 November 2018; accepted 17 March 2019;
https://doi.org/10.1016/j.omtn.2019.03.005.

[11]These authors contributed equally to this work.

Correspondence: Francis J. Miller, Jr., MD, Department of Medicine, Duke University, 508 Fulton St, Bldg. 15,Room 306, Durham, NC 27705, USA.
E-mail: francis.miller@duke.edu
Correspondence: Paloma H. Giangrande, PhD, Internal Medicine, University of Iowa, 375 Newton Rd., 5202 MERF, Iowa City, IA 52242, USA.
E-mail: paloma-giangrande@uiowa.edu
Correspondence: Saami K. Yazdani, PhD, Mechanical Engineering Department, University of South Alabama, 150 Jaguar Drive, Shelby Hall, Room 3123, Mobile, AL 36688, USA.
E-mail: syazdani@southalabama.edu

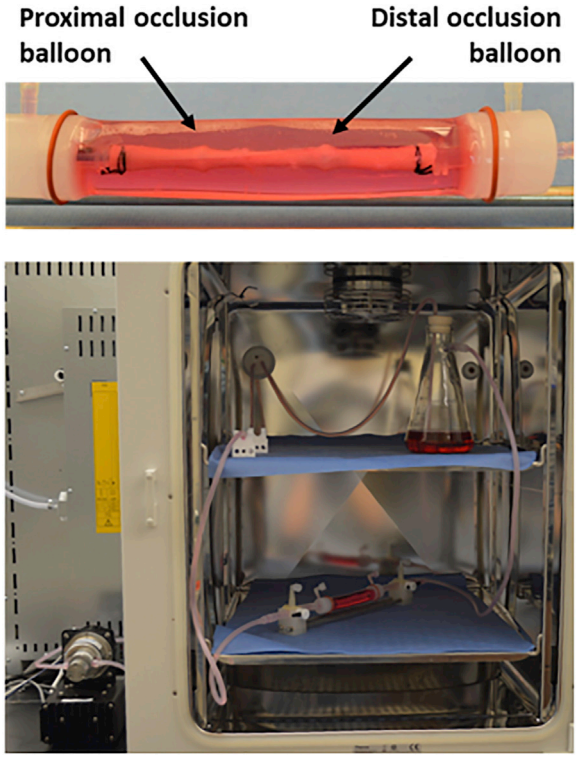

Figure 1. Schematic Diagram of the *Ex Vivo* Bioreactor System
Aptamer and controls were delivered to the explanted pig artery via the perfusion catheter. The specific treatment zone within the explanted pig arteries were between the proximal and distal occlusion balloons of the perfusion catheter. Following aptamer delivery, a computer-controlled gear pump generated and circulated culture medium at physiological flow rates. The treated artery and flow reservoir were housed within a CO_2 incubator.

binding affinities and specificities comparable to therapeutic antibodies and, due to their amenability to modification by medicinal chemistry, avoid immunogenicity concerns of protein-based drugs. RNA therapies are currently being developed and tested for ophthalmology,[14] coagulation (thrombosis),[15] oncology,[16] and inflammation.[17]

The purpose of this study was to determine the feasibility of delivery of a VSMC-specific bio-drug (RNA aptamer) directly to the medial wall via a novel catheter approach.[12,18] RNA aptamers are single-stranded oligonucleotides whose binding properties comparable to those of antibody and antigen interactions.[19,20] Here, we quantify the binding and retention of VSMC-specific aptamers delivered via a perfusion catheter.[21] We show the capability of the perfusion catheter to deliver aptamer directly to the medial layer and that delivery of VSMC-specific aptamers improves retention in the vessel wall as compared to control aptamer.

RESULTS

Visualization and Quantification of Fluorescent Signal

Figure 1 shows a representative image of a porcine carotid artery being treated by a perfusion catheter within the *ex vivo* bioreactor system. The explanted vessels (n = 3 per group; total of 24 arteries) were pulsed for 1 and 24 h while being subjected to physiological flow conditions and varying RNA aptamers. To visualize and quantify aptamer penetration, arteries were sectioned and visualized via confocal microscopy following 1- and 24-h post-delivery (Figure 2). Aptamer penetration was greatest for Apt01 as compared to Apt14, nonspecific control (NSC), and vehicle control at 1 h post-delivery (signal depth, 92.12 ± 32.45 μm versus 41.87 ± 24.10 μm versus 13.03 ± 7.79 μm versus 0.07 ± 0.06 μm, p = 0.003). At 24 h post-delivery, Apt14 showed the greatest depth penetration as compared to Apt01, NSC, and vehicle control (signal depth, 19.55 ± 3.96 μm versus 10.27 ± 1.52 μm versus 0.10 ± 0.00 μm versus 0.10 ± 0.00 μm, p < 0.0001). In comparing Apt01 and Apt14, both aptamers showed a loss in signal depth from 1 to 24 h post-delivery, although only the decrease in the Apt01 was significant (Apt01, 92.12 ± 32.45 μm versus 10.27 ± 1.52 μm, p < 0.0001; Apt14, 41.87 ± 24.10 μm versus 19.55 ± 3.96 μm, p = 0.210).

Similar patterns were also observed in the mean fluorescence measurements, as Apt01 showed greater levels at 1 h, followed by Apt14, NSC, and vehicle (mean fluorescence, 52.67 ± 17.86 optical density (OD) versus 16.30 ± 4.62 OD versus 2.97 ± 6.22 OD versus 0.00 ± 0.00 OD, p = 0.0006). At 24 h post-delivery, the fluorescence measurements reversed, and Apt14 was greater as compared to Apt01, NSC, and vehicle (mean fluorescence: 18.73 ± 7.73 OD versus 7.37 ± 1.44 OD versus 0.27 ± 0.42 OD versus 0.00 ± 0.00 OD, p = 0.0013). In comparing Apt01 and Apt14, the fluorescence of Apt14 remained similar between 1 and 24 h post-delivery (16.30 ± 4.62 OD versus 18.73 ± 7.73 OD, p = 0.999), whereas in Apt01, the fluorescence significantly decreased (52.67 ± 17.86 OD versus 7.37 ± 1.44 OD, p < 0.0001).

Ex Vivo RNA Aptamer Delivery

Aptamer tissue concentration was determined using both aptamer fluorescence binding and internalization (AFBI) assay[22] and qRT-PCR. At 1 h post-delivery, Apt01 showed higher arterial retention as compared to Apt14 and NSC (AFBI post-extraction, 1.880 ± 0.841 nM versus 1.409 ± 0.425 nM versus 1.165 ± 0.634 nM, p = 0.0277). However, at 24 h post-delivery, Apt14 had more retention as compared to Apt01 and NSC (AFBI post-extraction, 1.705 ± 0.783 nM versus 0.592 ± 0.191 nM versus 0.695 ± 0.275 nM, p = < 0.0001). In comparing Apt01 and Apt14 (Figure 3), Apt14 tissue levels remained similar between 1 and 24 h (1.409 ± 0.425 nM versus 1.705 ± 0.783 nM, p = 0.878), whereas in Apt01, tissue aptamer level decreased (1.880 ± 0.841 nM versus 0.592 ± 0.191 nM, p < 0.0001).

qRT-PCR analysis showed similar patterns to the AFBI assay. Retention of Apt01 was approximately 4-fold (3.995 ± 1.607-fold change) higher than the NSC control at 1 h, whereas Apt14 was equivalent to the NSC control (1.592 ± 0.328-fold change). However, at 24 h, fold change was greater for the Apt14 as compared to the NSC control versus Apt01 (3.37 ± 1.52-fold change versus 1.59 ± 0.33-fold change, p = 0.057). Additionally, a significant decrease in Apt01 was observed from 1 to 24 h (p = 0.0058) as shown in Figure 3.

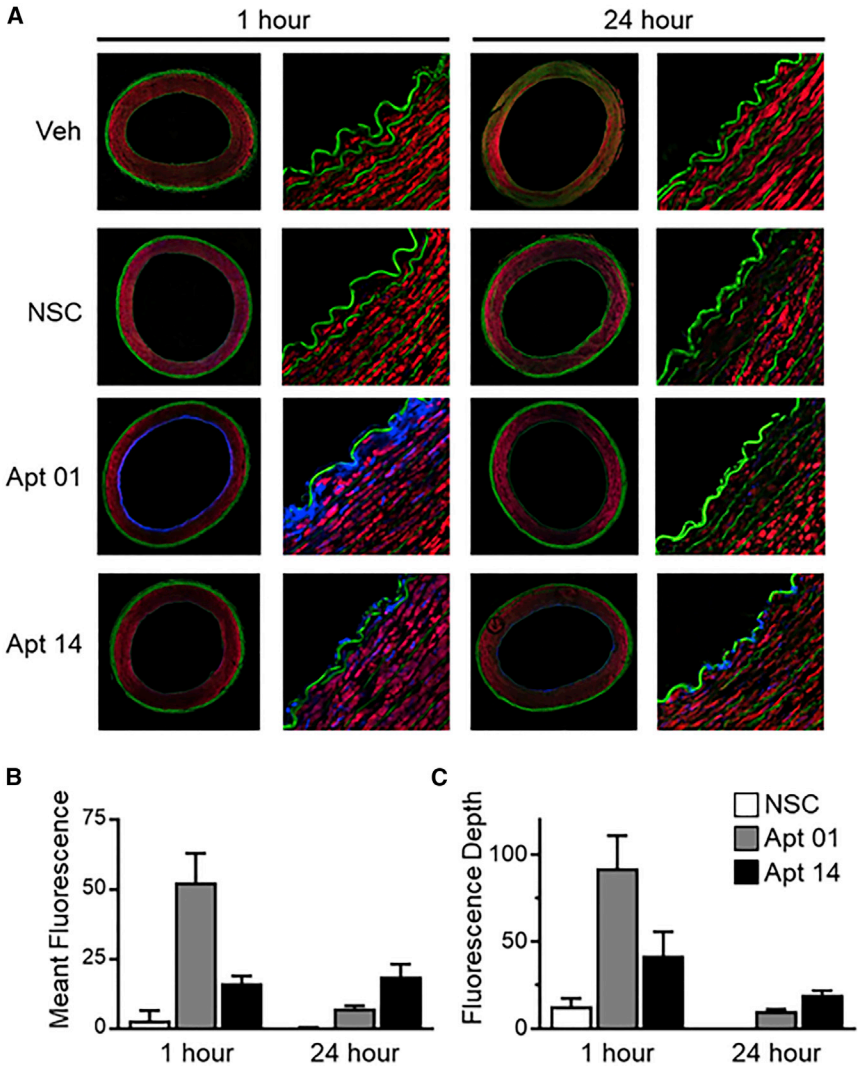

Figure 2. Confocal Microscopy Analysis of Aptamer Signals in Porcine Carotid from the 2-h Experiment
(A) Representative confocal images: Aptamers are visualized in blue, smooth muscle in red (phalloidin-Alexa Fluor 568), elastic fiber (auto-fluorescence) in green. High magnifications of boxed areas in panels in the left column are shown to the right side of each panel. Arrows indicate areas of prominent aptamer fluorescence. Scale bars, 1 mm for panels in the left column, 25 μm for panels in the right column. (B) Bar graph (with SE bars) showing normalized signal intensity in the wall of artery within 150 μm (the maximal signal depth of all) for each treatment. (C) Bar graph (with SE bars) representing signal depth of each treatment.

DISCUSSION

This study was designed to evaluate, for the first time, the delivery of cell-specific RNA aptamers directly into the medial layer of an intact artery using a perfusion catheter. Specifically, we compared two aptamers (Apt01 and Apt14) that were selected to bind to VSMCs against a control aptamer (NSC). The study was performed *ex vivo* using harvested swine carotid arteries under pulsatile flow conditions. The delivery and retention of the aptamer was evaluated at 1 and 24 h post-delivery, a critical time point to evaluate the potential success of therapeutic drugs delivered locally without the use of a permanent platform such as a stent.[21,23,24] Results demonstrated the delivery and retention of VSMC-specific aptamers were successful using the perfusion catheter. Confocal microscopy confirmed the presence of the aptamers within the medial region of the artery at 1 h post-delivery. A 24 h post-delivery, RNA aptamer Apt14 maintained similar tissue concentration and fluorescence as compared to 1 h, whereas RNA Apt01 (along with controls) decreased. These results suggest that Apt14 more selectively targets the arterial wall as compared to Apt01. Overall, this study demonstrates the capability of the perfusion catheter to deliver aptamer directly to the medial layer and that delivery of VSMC-specific aptamers improves retention in the vessel wall as compared to control aptamer.

The current therapeutic approach to inhibit restenosis following an endovascular procedure such as stenting or balloon angioplasty is to locally deliver anti-proliferative agents. However, devices such as drug eluting stents or drug-coated balloons universally delay and hinder the healing process.[9,10] Notably, since the anti-proliferative drugs such as paclitaxel and the limus family drugs are not specific to VSMCs, they target proliferating ECs and delay reendothelialization.[8] Bio-drugs, such as aptamers, can thus play a significant role in developing next-generation pro-healing therapeutic options, accelerating the healing of arteries and reducing the dependencies of anti-platelet therapy that minimize the thrombotic risks associated with incomplete reendothelialization.

For purposes of this study, we chose to test two aptamers (Apt01 and Apt14) that demonstrated high selective VSMC internalization and a control non-specific aptamer (NSC). Previously, we have shown that both Apt01 and Apt14 aptamers were distinct in sequence similarity and in structure similarity.[18] Specificity of the aptamers to VMSCs is performed by combining a cell-based selection method with high-throughput sequencing and bioinformatics analyses to rapidly identify cell-specific, internalization-competent RNA aptamers.[18] We have previously identified that Apt14 functions as a smart drug by inhibiting the phosphatidylinositol 3-kinase/protein kinase-B (P13K/Akt) and VSMC migration in response to multiple agonists by a mechanism that involves inhibition of platelet-derived growth factor receptor (PDGFR)-β phosphorylation.[12] The target of Apt01 still remains unknown and the focus of ongoing research.

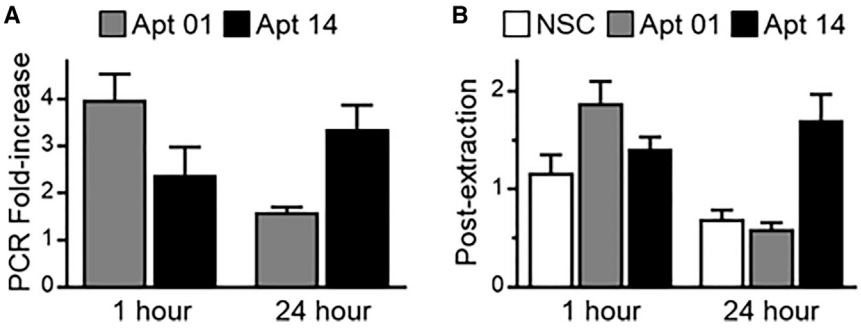

Figure 3. Measurement and Quantification of Recovered Aptamer

(A) Bar graph (with SE bars) showing fold increase in the recovery and quantification of aptamers 01 and 14 from pig carotids through RT-qPCR from the 1- and 24-h experiment using qRT-PCR. (B) Bar graph (with SE bars) showing measurement and quantification of NSC and aptamers 01 and 14 fluorescence post-extraction for the 1- and 24-h experiment using AFBI Assay.

We observed an overall trend of greater delivery and retention of Apt01 versus Apt14 at 1 h post-delivery; however, at 24 h, the trend is reversed, favoring Apt14. Significant loss in Apt01 from 1 to 24 h post-delivery is confirmed by confocal microscopy and aptamer tissue levels. The more favorable results of Apt01 at 1 h post-delivery suggest that Apt01 may have structural features that favor vascular wall penetration. The perfusion catheter delivers the aptamer by convection (rather than diffusion), pressurizing the treatment chamber and driving the aptamer across tissue layers into the medial wall. From previous studies using taxol,[21] factors that influence drug penetration include treatment chamber pressure, viscosity of the liquid drug, and severity of injury. In this study, all these factors were similar between the two groups (data not shown). Further studies are warranted to compare the structure of aptamers Apt01 versus Apt14.

At 24 h post-delivery, Apt14 maintained and showed greater tissue levels as compared to Apt01. The data thus suggest Apt14 is better retained either by greater affinity or enhanced internalization to VMSCs. Previously, we have shown that Apt14 can inhibit neointimal formation in a murine carotid injury model.[12] The aptamer was delivered to the injured artery via a peri-adventitial application of a pluronic gel (containing Apt14). The findings from this study indicate that the aptamer by itself has the potential to inhibit cellular processes. However, the delivery of aptamer using endovascular techniques provides a more suited clinical approach that can deliver aptamer in a minimally invasive manner. Furthermore, the local liquid delivery approach enables either a single aptamer or multiple aptamers concurrently delivered with complimentary function to inhibit vascular inflammation and VSMC growth. In addition, the construction of a chimera containing the aptamer and an siRNA or microRNA (miRNA) would allow SMC-specific delivery of these pathway modulators.

Limitations of this study include the fact that the aptamers utilized in this study were positively selected using murine VSMCs and not swine VSMCs.[18] And although the data seems to show cross-species reactivity, the purpose of this study was proof of principle, and species-specific aptamer selection may have resulted in improved retention and binding. Similar selection protocols can be implemented to identify aptamers that bind to pig or human SMCs and not to ECs. An additional limitation is that our *ex vivo* system used culture medium as the working fluid rather than whole blood and utilized healthy (non-diseased) arteries, although we have shown that Apt 14 has a half-life of 300 h in human serum.[12]

Conclusions

This study provides first evidence of the use of a perfusion catheter to directly deliver RNA aptamer into the medial wall and that delivery of VSMC-specific aptamers improves retention in the vessel wall as compared to control aptamer. Further studies are warranted to demonstrate the safety and efficacy profile of the aptamer *in vivo* with comparisons to current gold standards. Overall though, such specific targeted therapeutic drugs provide a potentially safer and more effective treatment option for patients with vascular disease.

MATERIALS AND METHODS

RNA Aptamers

RNA aptamers were either chemically synthesized (5′C12-NH2, 5′ biotin C12-NH) by TriLink Biotechnologies (San Diego, CA, USA) or generated by *in vitro* transcription with 2′-fluoro pyrimidines and 2′-OH purines. The *in vitro* transcription was performed using the Y639F mutant T7 RNAP (obtained from Dr. Rui Sousa, University of Texas, San Antonio, TX, USA) on double-stranded DNA (dsDNA) from extended single-stranded DNA (ssDNA) template oligos as previously reported.[12,18] The ssDNA templates were synthesized by Integrated DNA Technologies (IDT; Coralville, IA, USA) at 25 nmol/L scale with desalting purification and no modifications as follows:

aptamer 14 5′-TCGGGCGAGTCGTCTGGGGAGGTCAGAACGAAAGGCCCGCATCGTCCTCCC-3′,

aptamer 01 5′-GGGAGGACGAUGCGGUCCUGUCGUCUGUUCGUCCCCAGACGACUCGCCCGA-3′,

aptamer NSC 5′-TCGGGCGAGTCGTCTGCGAGGCAACAAGCTCGTAATCCGCATCGTCCTCCC-3′.

Synthetic and *in vitro* transcribed RNA aptamers were folded at 3 μmol/L concentration using the following protocol: 5 min 95°C, 15 min 65°C, and 20–30 min 37°C. The folded aptamer RNA was diluted to 150 nmol/L in full media.

Ex Vivo Bioreactor System

Twenty-four porcine carotid arteries were harvested from large pigs (110–160 kg) from a local abattoir (Semmes, AL, USA) and transferred

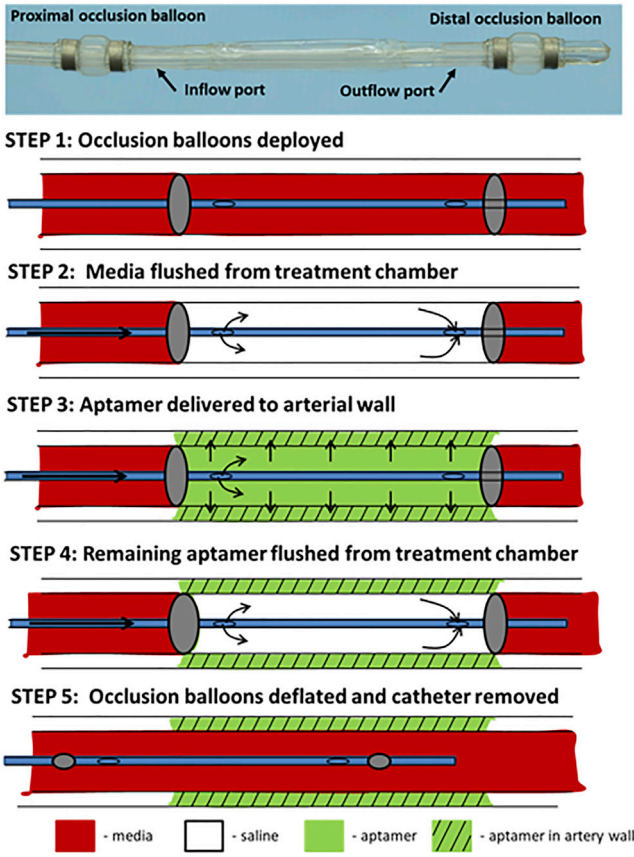

Figure 4. Schematic Illustration of the Perfusion Catheter

Two occluding balloons are deployed to momentarily stop circulating flow to a portion of a vessel. Trapped blood within the perfusion chamber is then flushed with saline. Drug can be delivered through the inflow port. The outflow port can be closed and drug delivered to the lesion with external pressure. The delivery pressure is measured by a fiberoptic pressure sensor located at the inlet port. Following the delivery of the drug, the remaining drug in the chamber is cleared through the outflow port to ensure no additional drug is introduced into the circulatory system.

in sterile PBS with 1% antibiotic-antimycotic (Gibco, Grand Island, NY, USA). Vessels were then rinsed in sterile PBS in a culture hood. The excess fat, connective tissue, and fascia were removed from each vessel. Vessels were cut into approximately 8-cm segments and stored in 15-mL centrifuge tubes at −20°C until needed. Frozen vessels were thawed in a 37°C water bath and placed into the bioreactor system to be studied.

The bioreactor system used in this study consisted of a flow reservoir, pump, vessel housing compartment, and a distal flow constrictor, as described previously.[21] In brief, the pressure was monitored via a catheter pressure transducer (Millar Instruments, Houston, TX, USA). The flow was monitored by an ultrasonic flow meter (Emtec flow technology, Berkshire, NY, USA) that was positioned prior to the bioreactor. A custom LabVIEW program was used to generate pulsatile waveforms and to control and monitor the mechanical conditions (flow and pressure) within the bioreactor system. The bioreactor medium consisted of DMEM containing low glucose, (1,000 mg/L), 4.0 mM L-glutamine, 110 mg/L sodium pyruvate, pyridoxine hydrochloride, 10% fetal bovine serum (Gibco), and 1% antibiotic-antimycotic (Gibco).

To deliver aptamer locally to selected regions, a multi-lumen balloon perfusion catheter (Advanced Catheter Therapies, Chattanooga, TN, USA) was utilized. Prior to aptamer delivery, *ex vivo* arteries underwent endothelial denudation using an angioplasty balloon catheter (5.0 mm × 15 mm). The perfusion catheter can temporarily occlude the target area from blood flow by deploying occlusion balloons (Figure 4). The treatment chamber can then be flushed to remove trapped circulating media. Following flushing of the treatment chamber, the aptamer was delivered to the treatment chamber. The delivery of aptamer is accomplished by pressure differences created by an increase in luminal pressure by the perfusion catheter thereby driving the aptamer across tissue layers into the medial wall. Aptamers were delivered at a final concentration of 250 nM for 2 min. Following delivery, the treated arteries were exposed to physiological flow conditions for either 1 or 24 h.

AFBI Assay

Figure 5 provides the overall approach of quantifying the RNA aptamers. Following perfusion with RNA aptamers, each arterial segment was placed in a 400 μg/mL proteinase K (QIAGEN, 19131) lysis buffer (100 nmol/L NaCl, 10 mmol/L Tris-HCl [pH 8.0], 0.5% SDS) and incubated overnight at 55°C. The resulting solution was measured for fluorescence intensity before and after RNA aptamer was extracted using a miRCURY RNA tissue isolation kit (EXIQON, 300111) from the lysed proteinase K samples. Then, 10 μL of each sample was added × 4 into a 384-well plate (Nunc, black flat bottom), and the absorbance measured at a wavelength of between 640 and 670 nM.

qRT-PCR Assay

Following perfusion with RNA aptamers, the RNA was extracted from each arterial segment using a miRCURY RNA tissue isolation kit (EXIQON, 300111) with several modifications. The proteinase K (QIAGEN, 19131) and lysis buffer (100 nmol/L NaCl, 10 mmol/L Tris HCl [pH 8.0], 0.5% SDS) used was not from the miRCURY RNA tissue isolation kit (EXIQON, 300111). Each arterial segment (25mg) was placed in a 400 μg/mL proteinase K (QIAGEN, 19131), 250μL lysis buffer (100 nmol/L NaCl, 10 mmol/L Tris HCl [pH 8.0], 0.5% SDS) and incubated overnight at 55°C, even though the kit recommended 15 min incubation. Also during incubation, the lysate was spiked with a known quantity of Sel1 processing control aptamer (M12-23), then the extraction steps were followed as outlined in the miRCURY RNA tissue isolation kit (EXIQON, 300111). The recovered RNA aptamer was quantified by qRT-PCR using Power SYBR Green PCR Mastermix (Applied Biosystems, 4367659) and as outlined previously.[25] We performed two independent RT and PCR reactions for each RNA sample, one with the

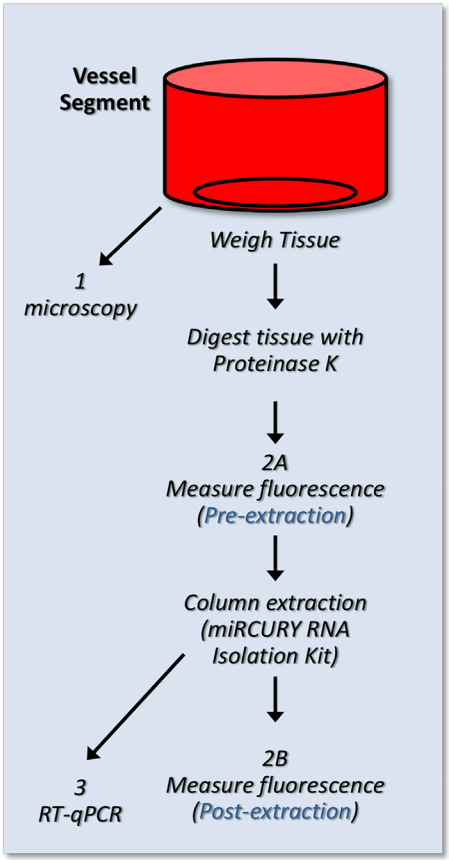

Figure 5. Schematic Illustration of Vessel Processing

Schematic diagram illustrating the RNA perfusion of vessel and processing for RNA quantification and imaging.

Sel1 primers (Sel1 PCR) and one with the Sel2 primers (Sel2 PCR). The Sel1 PCR was used as a normalization control for sample processing. Proper processing is confirmed by similar Sel1 PCR values (cyclic threshold [CT] values) for each sample. Any samples that are excessively low or high were flagged as possibly problematic due to extraction error.

Confocal Microscopy

Histochemistry

Five-millimeter sections obtained from the perfused carotid arteries were fixed in 4% paraformaldehyde (Affymetrix, Santa Clara, CA, USA) at 4°C for 5 h, cryo-protected in 30% sucrose in PBS at 4°C overnight, and then quick-froze on dry ice. Frozen 20-μm coronal sections were cut with a cryostat (Thermo Scientific HM550) and mounted on Colorfrost Plus microscope slides (Fisher Scientific, Hampton, NH, USA). Sections were stained with phalloidin-Alexa Fluor 568 (Thermo Fisher Scientific) to visualize smooth muscle in the carotid artery. Stained sections were covered using coverslips and Prolong Diamond Anti-Fade Reagents (Invitrogen, Carlsbad, CA, USA) after washed with PBS.

Imaging

Fluorescently stained slides were examined with a Zeiss LSM 710 confocal laser scanning microscope. Sections were scanned sequentially in different channels to separate labels. Images from different channels were each assigned a pseudo-color and then were superimposed. Confocal images were obtained and processed with software provided with the Zeiss LSM 710.

Image Analysis

The NIH ImageJ software, a public domain program available from the NIH (https://imagej.nih.gov/ij/), was used to analyze confocal images. Signal depth (from lumen into the muscle layer) was estimated from 10 measurements performed on three independent vessel segments with each treatment condition. Mean fluorescence was obtained from the signal intensity of five randomly selected areas from three independent vessel segments for each treatment condition.

Statistical Analysis

Results are expressed as mean ± SEM. Statistical comparisons were performed by ANOVA using GrapPad Prism 7 (GraphPad Software, La Jolla, CA, USA). Comparison of multiple groups was performed by Tukey's multiple comparisons post hoc test. A value of $p < 0.05$ was considered statistically significant.

AUTHOR CONTRIBUTIONS

Writing – Original Conceptualization, P.H.G., S.K.Y., F.J.M.; Methodology, O.U., P.H.G., L.-H.L., S.K.Y.; Data Acquisition, Curation, and Analysis, O.U., L.-H.L., F.J.M., P.H.G., E.T., M.E., S.K.Y.; Resources, P.H.G., S.K.Y.; Writing – Draft, S.K.Y., O.U., L.-H.L.; Writing – Review and Editing, O.U., S.K.Y., F.J.M., P.H.G., L.-H.L.; Supervision, P.H.G. and S.K.Y.

CONFLICTS OF INTEREST

S.K.Y. has received grant support from Lutonix, Inc., Advanced Catheter Therapies, and Toray Industries. All other co-authors declare no conflict of interest regarding the publication of this article.

ACKNOWLEDGMENTS

The authors would like to acknowledge the Iowa City VA Medical Center for the use of equipment (cryostat and confocal microscope). This work was funded by the University of Iowa Carver College of Medicine (CCOM) (Carver Collaborative Pilot Grant Award 2015), the University of Iowa Award from The Office of the Vice President for Research and Economic Development (OVPRED 2015), and retention funds from the University of Iowa Department of Internal Medicine. P.H.G. is supported by the NIH (R01CA138503 and R21DE019953), the Mary Kay Foundation (9033-12 and 001-09), the Elsa U. Pardee Foundation (E2766), and the Roy J. Carver Charitable Trust (RJCCT 01-224). O.U. is supported by a postdoctoral NIH training grant (T32HL007121-41). W.H.T. is supported by the American Heart Association (14SDG18850071). F.J.M. is supported by the Office of Research and Development, Department of Veterans Affairs (2I01BX001729), and the NIH (HL130039). S.K.Y. is supported by the American Heart Association (15SDG25880000) and

NIH (1R15HL127596). E.T. is supported by a predoctoral American Heart Association grant (16PRE27350003). The data that support the findings of this study are available from the corresponding authors upon reasonable request.

REFERENCES

1. Benjamin, E.J., Blaha, M.J., Chiuve, S.E., Cushman, M., Das, S.R., Deo, R., de Ferranti, S.D., Floyd, J., Fornage, M., Gillespie, C., et al.; American Heart Association Statistics Committee and Stroke Statistics Subcommittee (2017). Heart Disease and Stroke Statistics-2017 Update: A Report From the American Heart Association. Circulation *135*, e146–e603.
2. Gerhard-Herman, M.D., Gornik, H.L., Barrett, C., Barshes, N.R., Corriere, M.A., Drachman, D.E., Fleisher, L.A., Fowkes, F.G.R., Hamburg, N.M., Kinlay, S., et al. (2017). 2016 AHA/ACC Guideline on the Management of Patients With Lower Extremity Peripheral Artery Disease: A Report of the American College of Cardiology/American Heart Association Task Force on Clinical Practice Guidelines. J. Am. Coll. Cardiol. *69*, e71–e126.
3. Al Suwaidi, J., Berger, P.B., and Holmes, D.R., Jr. (2000). Coronary artery stents. JAMA *284*, 1828–1836.
4. Guagliumi, G., Virmani, R., Musumeci, G., Motta, T., Valsecchi, O., Bonaldi, G., Saino, A., Tespili, M., Greco, N., and Farb, A. (2003). Drug-eluting versus bare metal coronary stents: long-term human pathology. Findings from different coronary arteries in the same patient. Ital. Heart J. *4*, 713–720.
5. Axel, D.I., Kunert, W., Göggelmann, C., Oberhoff, M., Herdeg, C., Küttner, A., Wild, D.H., Brehm, B.R., Riessen, R., Köveker, G., and Karsch, K.R. (1997). Paclitaxel inhibits arterial smooth muscle cell proliferation and migration in vitro and in vivo using local drug delivery. Circulation *96*, 636–645.
6. Stone, G.W., Ellis, S.G., Cox, D.A., Hermiller, J., O'Shaughnessy, C., Mann, J.T., Turco, M., Caputo, R., Bergin, P., Greenberg, J., et al.; TAXUS-IV Investigators (2004). A polymer-based, paclitaxel-eluting stent in patients with coronary artery disease. N. Engl. J. Med. *350*, 221–231.
7. Morice, M.C., Serruys, P.W., Sousa, J.E., Fajadet, J., Ban Hayashi, E., Perin, M., Colombo, A., Schuler, G., Barragan, P., Guagliumi, G., et al.; RAVEL Study Group. Randomized Study with the Sirolimus-Coated Bx Velocity Balloon-Expandable Stent in the Treatment of Patients with de Novo Native Coronary Artery Lesions (2002). A randomized comparison of a sirolimus-eluting stent with a standard stent for coronary revascularization. N. Engl. J. Med. *346*, 1773–1780.
8. Otsuka, F., Finn, A.V., Yazdani, S.K., Nakano, M., Kolodgie, F.D., and Virmani, R. (2012). The importance of the endothelium in atherothrombosis and coronary stenting. Nat. Rev. Cardiol. *9*, 439–453.
9. Vorpahl, M., Yazdani, S.K., Nakano, M., Ladich, E., Kolodgie, F.D., Finn, A.V., and Virmani, R. (2010). Pathobiology of stent thrombosis after drug-eluting stent implantation. Curr. Pharm. Des. *16*, 4064–4071.
10. Joner, M., Finn, A.V., Farb, A., Mont, E.K., Kolodgie, F.D., Ladich, E., Kutys, R., Skorija, K., Gold, H.K., and Virmani, R. (2006). Pathology of drug-eluting stents in humans: delayed healing and late thrombotic risk. J. Am. Coll. Cardiol. *48*, 193–202.
11. Nakazawa, G., Otsuka, F., Nakano, M., Vorpahl, M., Yazdani, S.K., Ladich, E., Kolodgie, F.D., Finn, A.V., and Virmani, R. (2011). The pathology of neoatherosclerosis in human coronary implants bare-metal and drug-eluting stents. J. Am. Coll. Cardiol. *57*, 1314–1322.
12. Thiel, W.H., Esposito, C.L., Dickey, D.D., Dassie, J.P., Long, M.E., Adam, J., Streeter, J., Schickling, B., Takapoo, M., Flenker, K.S., et al. (2016). Smooth Muscle Cell-targeted RNA Aptamer Inhibits Neointimal Formation. Mol. Ther. *24*, 779–787.
13. Zhou, J., and Rossi, J. (2017). Aptamers as targeted therapeutics: current potential and challenges. Nat. Rev. Drug Discov. *16*, 440.
14. Drolet, D.W., Green, L.S., Gold, L., and Janjic, N. (2016). Fit for the Eye: Aptamers in Ocular Disorders. Nucleic Acid Ther. *26*, 127–146.
15. Staudacher, D.L., Putz, V., Heger, L., Reinöhl, J., Hortmann, M., Zelenkofske, S.L., Becker, R.C., Rusconi, C.P., Bode, C., and Ahrens, I. (2017). Direct factor IXa inhibition with the RNA-aptamer pegnivacogin reduces platelet reactivity in vitro and residual platelet aggregation in patients with acute coronary syndromes. Eur. Heart J. Acute Cardiovasc. Care. Published online April 13, 2017. 10.1177/2048872617703065.
16. Reyes-Reyes, E.M., Teng, Y., and Bates, P.J. (2010). A new paradigm for aptamer therapeutic AS1411 action: uptake by macropinocytosis and its stimulation by a nucleolin-dependent mechanism. Cancer Res. *70*, 8617–8629.
17. Oberthür, D., Achenbach, J., Gabdulkhakov, A., Buchner, K., Maasch, C., Falke, S., Rehders, D., Klussmann, S., and Betzel, C. (2015). Crystal structure of a mirror-image L-RNA aptamer (Spiegelmer) in complex with the natural L-protein target CCL2. Nat. Commun. *6*, 6923.
18. Thiel, W.H., Bair, T., Peek, A.S., Liu, X., Dassie, J., Stockdale, K.R., Behlke, M.A., Miller, F.J., Jr., and Giangrande, P.H. (2012). Rapid identification of cell-specific, internalizing RNA aptamers with bioinformatics analyses of a cell-based aptamer selection. PLoS ONE *7*, e43836.
19. Thiel, K.W., and Giangrande, P.H. (2009). Therapeutic applications of DNA and RNA aptamers. Oligonucleotides *19*, 209–222.
20. Keefe, A.D., Pai, S., and Ellington, A. (2010). Aptamers as therapeutics. Nat. Rev. Drug Discov. *9*, 537–550.
21. Atigh, M.K., Turner, E., Christians, U., and Yazdani, S.K. (2017). The use of an occlusion perfusion catheter to deliver paclitaxel to the arterial wall. Cardiovasc. Ther. *35*, 35.
22. Thiel, W.H., and Giangrande, P.H. (2016). AFBI assay - Aptamer Fluorescence Binding and Internalization assay for cultured adherent cells. Methods *103*, 180–187.
23. Yazdani, S.K., Pacheco, E., Nakano, M., Otsuka, F., Naisbitt, S., Kolodgie, F.D., Ladich, E., Rousselle, S., and Virmani, R. (2014). Vascular, downstream, and pharmacokinetic responses to treatment with a low dose drug-coated balloon in a swine femoral artery model. Catheter. Cardiovasc. Interv. *83*, 132–140.
24. Fernandez-Parra, R., Laborda, A., Lahuerta, C., Lostalé, F., Aramayona, J., de Blas, I., and de Gregorio, M.A. (2015). Pharmacokinetic Study of Paclitaxel Concentration after Drug-Eluting Balloon Angioplasty in the Iliac Artery of Healthy and Atherosclerotic Rabbit Models. J. Vasc. Interv. Radiol. *26*, 1380–1387.e1.
25. Thiel, W.H., Thiel, K.W., Flenker, K.S., Bair, T., Dupuy, A.J., McNamara, J.O., 2nd, Miller, F.J., and Giangrande, P.H. (2015). Cell-internalization SELEX: method for identifying cell-internalizing RNA aptamers for delivering siRNAs to target cells. Methods Mol. Biol. *1218*, 187–199.